AAS 93-165

VERY-LONG-BASELINE-INTERFEROMETRY MEASUREMENTS OF PLANETARY ORBITERS AT MARS AND VENUS

Peter M. Kroger, William M. Folkner,
Byron A. Iijima and Claude E. Hildebrand

Very-long-baseline interferometric (VLBI) measurements of the positions of planetary orbiters (or landers) relative to nearby extra galactic radio sources provide information on the positions of the planets in the inertial reference frame described by the measured positions of the radio sources. This information is important for interplanetary spacecraft navigation by radio frequency techniques since it establishes the relationship between the reference frame of the target planets with the reference frame in which the spacecraft position measurements are made. Any angular offset between the two reference frames will result in a systematic error in the planet relative angular position of the spacecraft.

The first attempts to use radio interferometric techniques to measure the positions of planetary orbiters were made in 1980 with the Viking Mars orbiter and again in 1983 using the Pioneer Venus orbiter. The angular accuracy of these early measurements was on the order of 200 nrad. This work describes more recent VLBI measurements made in 1989 of the Soviet Martian orbiter, Phobos 2, and several measurements made since September of 1990 of the Magellan spacecraft orbiting Venus. Both the Phobos and Magellan measurements recorded data with the Mark III VLBI systems located at antennas of NASA's Deep Space Network (DSN). The much wider bandwidth of this recording system and the availability of ionospheric calibrations should allow angular accuracy approaching 10 nrad to be achieved with these measurements

INTRODUCTION

Very long baseline. interferometry (VI .BI) provides very precise information on the angular position of interplanetary spacecraft in the reference frame of extra galactic radio sources (quasars). Current VI .BI systems now in place at NASA's Deep Space Network (DSN) stations have the capability to measure spacecraft angular positions with an accuracy of 5 nrad. When combined with Doppler and range measurements, the full 6 dimensional spacecraft state vector can be estimated. This information is crucial during the. cruise and planetary approach phase of e.very mission. After a spacecraft has entered the orbit phase of its mission, Doppler data alone are. often sufficient to meet mission navigation requirements. Nevertheless, VI .BI measurements of orbiters provide valuable information on the relationship between the reference frames of the extragalactic radio sources and the planetary ephemerides that is of benefit to all interplanetary missions.

This paper describes a number of VLBI measurements that have been completed on two planetary orbiters: the Soviet Phobos 2 Martian orbiter launched in 1988, and NASA's Magellan spacecraft launched in 1989 to complete a molar map of the surface of Venus.

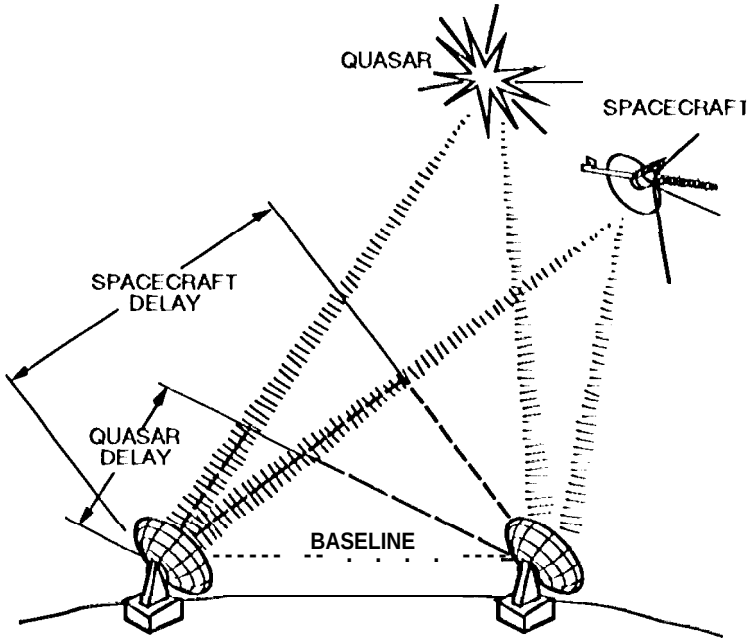

Figure 1. Observation geometry for AVLBI measurements of spacecraft.

VLBI MEASUREMENTS OF INTERPLANETARY SPACECRAFT

The primary observable in interferometric measurements is the relative delay difference, $\Delta\tau$, between the times of arrival of the spacecraft and quasar signals at two receiving antennas as shown in Figure 1. This delay difference is related to the baseline vector, **B**, and the unit vectors in the directions of the spacecraft, $\hat{\mathbf{s}}_{sc}$ and the extragalactic radio source (egrs), $\hat{\mathbf{s}}_{egrs}$ by

$$\Delta\tau = -\frac{\mathbf{B}\cdot\left(\hat{\mathbf{s}}_{sc} - \hat{\mathbf{s}}_{egrs}\right)}{c} \qquad (1)$$

where c is the speed of light.

The *a priori* positions of the radio sources used in the of the Phobos 2 and Magellan observations are known with an accuracy of 5 nrad or better from analysis of several years of repeated VLBI astrometry measurements carried out by both DSN and other antennas.1 These same VLBI measurements of the source positions also provide estimates of the baseline vector coordinates with an accuracy of several centimeters. Since the source positions and the baseline vector are known from these independent measurements, the observed delay difference of Eq.(1) allows the position of the spacecraft to be determined in the reference frame of the quasars. If the angular position of the quasar is close to that of the spacecraft, many common media errors will cancel when the differenced delay observable is formed.

DATA ACQUISITION

Observation summary

The Phobos 2 orbiter VI BI observations consist of two independent measurement sessions on Feb. 17, 1989 and March 25, 1989. The spacecraft was lost shortly after the second measurement and its signal was never reacquired. To date there have been four successful observations of the Magellan spacecraft since. it entered Venus orbit in Aug. 1990. VLBI measurements of Magellan will continue through the end of the mission in May of 1993. Table 1 summarizes the. VLBI measurements of Phobos and Magellan discussed in this paper.

Table 1
VLBI OBSERVATIONS OF PLANETARY ORBITERS

Spacecraft	Date	Observing Stations	Quasars	$\Delta\Theta$,deg*
Phobos 2	Feb. 17, 1989	DSS 14/DSS 63/ Jodrell Bank	0317+188	5.6
			0250+178	1.0
			0235+164	4.8
Phobos 2	Mar, 25, 1989	DSS 14/DSS 43	0426+273	4.4
			0409+229	3.2
			0423+233	0.4
Magellan	Sep. 12, 1990	DSS 13/DSS 45	OL 064.5	4.0
			P 1123+26	20.2
Magellan	Dec. 21, 1991	DSS 13/DSS 45	P 1504-167	1.7
			P 1510-08	6.2
Magellan	Dec. 22,1991	DSS 13/DSS 43	P 1504-167	2.3
			P 1510-08	6.5
Magellan	Mar, 29, 1992	DSS 15/DSS 43	P 2320-035	2.0

*Minimum separation angle between spacecraft and quasar.

Recording system

Both the Phobos 2 and Magellan observations used the Mark 111 (or wide channel bandwidth (WCB)) recording system now in place at all DSN tracking stations. 'I'his system allows data to be recorded in up to 14 independent channels, each with a nominal 2 MHz bandwidth (recording rate 4 Mbits/channel). The channels may be placed anywhere within the IF bandpass of the receiving system. For spacecraft measurements, certain channels arc allocated to record spacecraft tones while the remaining channels are devoted to recording the broadband quasar signal,

in the case of the Phobos 2 observations, the. spacecraft signal consisted of odd harmonics of a 7.4 MHz square wave modulated onto the 1.7 GHz carrier. Only the +/- 1st and -3rd harmonics provided adequate signal to noise ratio for these measurements. Each spacecraft tone was recorded in a pair of channels as a safeguard against channel failure. These channel pairs were also offset in frequency to provide information on instrumental phase effects in the VLBI recording system. Figure 2 shows the entire Mark III channel configurate ion used for the Phobos 2 observations.

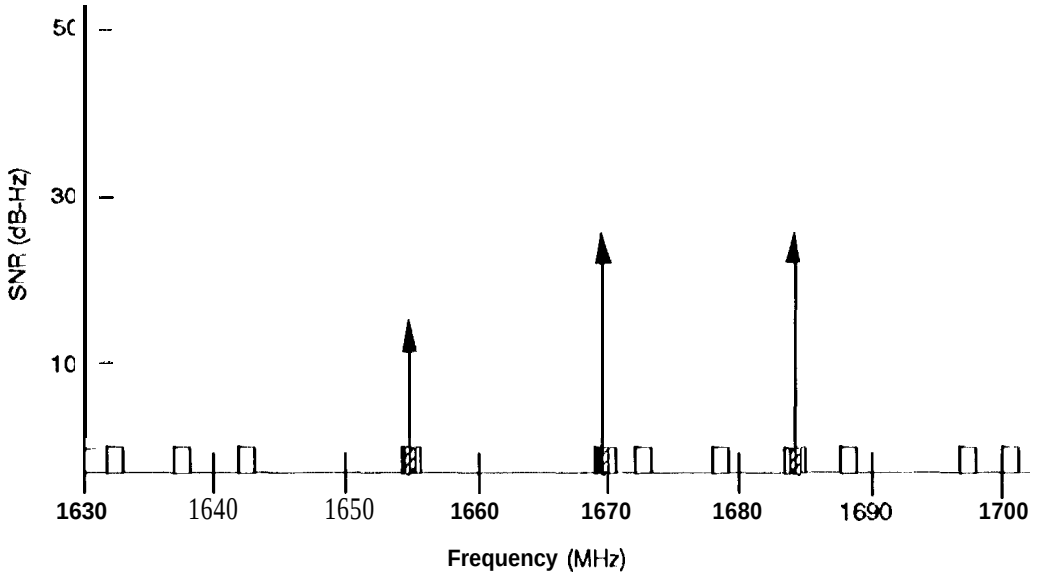

Figure 2. Channel configuration used for VLBI measurements of the Phobos 2 spacecraft. The rectangles represent the 14, 1.8 MHz channels of the Mark III VLBI recording system. The vertical arrows represent the location and signal to noise ratio of the spacecraft tones recorded during these observations.

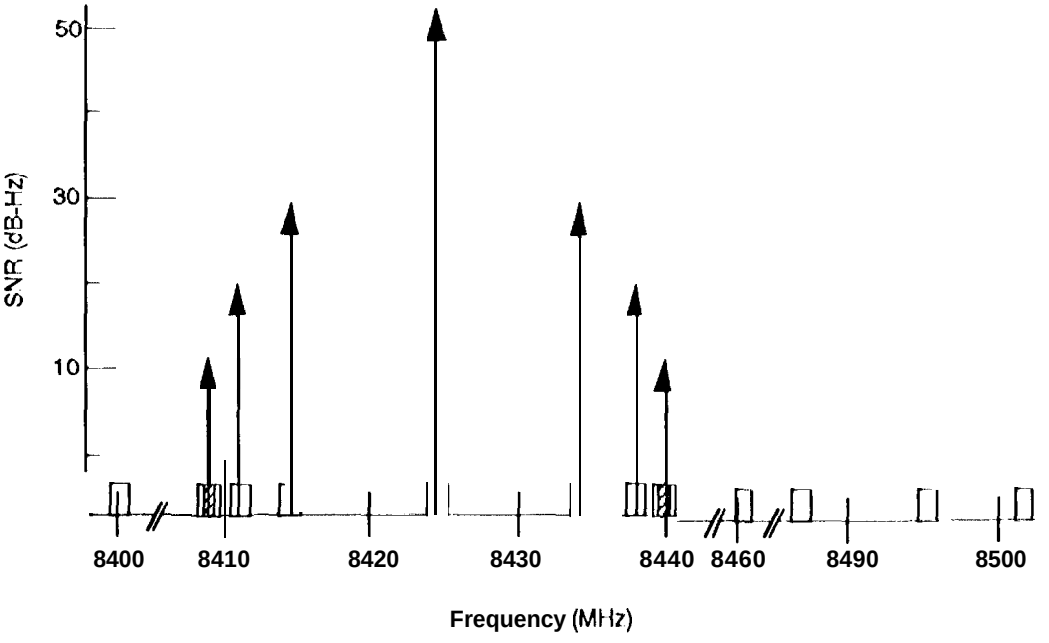

Figure 3. Channel configuration used for Magellan spacecraft observations. Each rectangle represents a single 1.8 MHz channel. The vertical arrows represent the location and signal to noise ratio of the spacecraft tones. The central tone is the carrier and the other tones are harmonics of a 960 kHz subcarrier used for transmission of radar mapping data.

The telemetry system on the Magellan spacecraft consists of an 8.4 GHz carrier signal which can be modulated by one of 3 subcarrier frequencies. The subcarriers produce a spectrum of tones whose even harmonics arc separated by a constant frequency. The two subcarriers used for the Magellan VLBI observations had tone separations of either 960 kHz or 360 kHz. A typical channel configuration for a Magellan VLBI observation using the 960 kHz subcarrier is shown in Fig. 3.

DATA ANALYSIS

Correlation

The tapes containing the recorded spacecraft and quasar signals are shipped to JPL where they are processed at the JPL/Caltech Block 11 VLBI correlator. Processing of the broadband quasar signals proceeds in the same manner as any astronomical VLBI measurement of a radio source[2]. 'l'he recorded data are played back through the correlator where the data streams from the. two stations are multiplied, The result of this multiplication is heterodyned to near zero frequency by multiplication with a phase model generated in the correlator. The resulting low frequency signal is averaged over 2 second intervals and written to a file for further processing, The initial clock offset used is determined by cm-relating the data streams at a number of relative delays. The clock offset is set to the dela y which produces the largest amp] it ude output.

The. spacecraft data consist of all the tones recorded in the individual channels of the Mark III system. The correlation of these data proceeds differentl y in that the data recorded at the two stations arc not multiplied together as in the case of the. quasar data, but are multiplied by an accurate phase. model for each station and tone to produce near zero frequency outputs which are then differenced between stations to form a quantity analogous to the quasar correlation output,

Post processing

"l'he correlation process described above produces a set of amplitudes and phases at 2 second intervals for all 14 channels of the quasar data and for every channel in which a spacecraft tone was recorded (actually a set of phases is produced for 8 discrete frequencies within each of the 14 channels). These phases are actually the difference between the correlator mode] phase and the actual total measured phase and hence forth will be referred to as residual phases. These residual phases contain all of the information on the relative delay of the spacecraft and quasar signals that will ultimately be used to estimate the angular separation between them (Eq. (1)). The next stage of the processing combines the data from all channels to finally produce a single group delay observable for each spacecraft and quasar scan. As part of this process, the data are calibrated to remove the effects introduced by the receiving system on the phase of the spacecraft and quasar signals.

Phase compression. The residual phases produced by the corrc.later at 2 second intervals for each channel are fit to a linear model

$$\phi_\alpha(\omega_i, t_j) = \Phi_\alpha(\omega_i) + \omega_i f(t_j) + \sigma_\alpha(\omega_i, t_j) \qquad (2)$$

where ϕ_α is the phase in channel α, frequency ω_i and at time t_j. The intercept Φ_α is the phase for channel α at frequency ω_i. $f(t_j)$ contains all of the information on the temporal fluctuations and drifts, and σ_α is an estimate of the system noise of the residual phase obtained in the correlation process and is used as a data weight in the linear fit to estimate Φ_α. The compressed phase@., is then passed to the next stage of processing where it is calibrated for the effects of the receiving system instrumental ion.

Phase calibration. The compressed residual phase for each channel produced in the previous stage of processing contains contributions from the receiving system electronics which must be removed to avoid introduction of a serious systematic error into the results. In the case of the Phobos 2 observations the correlation results from a strong quasar scan are used to estimate the nonlinear component of the instrumental phase. This phase calibration is then applied to the spacecraft scans by interpolation to the spacecraft tone frequency.

Computation of group delay. The residual phases from all channels, calibrated to remove the effects of the receiving system instrumentation, are combined to form a single group delay observable for each scan. The residual phases from each channel are fit to a linear model in frequency.

$$\Phi_\alpha(\omega_i) = \Phi_\alpha^o + \tau_r^g \omega_i + \sigma_\alpha^s(\omega_i) + \sigma_\alpha^p(\omega_i) \qquad (3)$$

The estimated slope of this fit, τ_g^r, is the residual group delay observable. σ_α^s is the error due to system noise effects and σ_α^p is the error in the. instrumental phase calibration.

Mode] restoration. The delay models used in the correlation are evaluated at the. scan reference time and added to the residual group delay computed in the previous stage to form the total group delay observable. These quantities, computed for each quasar and spacecraft scan, then form the input to the final stage of processing where the actual angular separation between the spacecraft and quasar are estimated.

ERROR ANALYSIS

Many of the error sources which contribute to the total error in AV1 .BI spacecraft measurements are strongly dependent on the observing geometry and can change markedly between observations and even during the course of a single measurement. In addition, quantities such as the signal to noise ratio of the quasar signal depend strongly on the brightness of the particular source that is observed. The received spacecraft signal strength also changes as the distance to Earth varies throughout the year. For these. reasons it is difficult to present a single error budget that is applicable to all AVLBI measurements even for a single spacecraft.

Rather than attempt this, we present in Figures 4 and 5 error budgets for two particular AVLBI measurements of the Phobos 2 and Magellan spacecraft. One of the primary differences between the error budgets for the two spacecraft arises from the different transmitted frequencies. The I.-band transmissions of the Phobos 2. spacecraft arc affected to a much greater extent by the ionosphere than the X-band transmissions of the Magellan spacecraft. The error budgets in Figures 4 and S do not include any systematic errors that affect the overall navigation budget. Primary among these are uncertainties in the planetary positions relative to Earth and in the relationship between the reference system of the planetary ephemerides and the reference system of the quasars. Indeed it is the intended purpose of these measurements to improve our

knowledge of these systematic effects. The remainder of this section provides a brief description of the major error sources affecting the ΔVI .131 measurements for the two spacecraft.

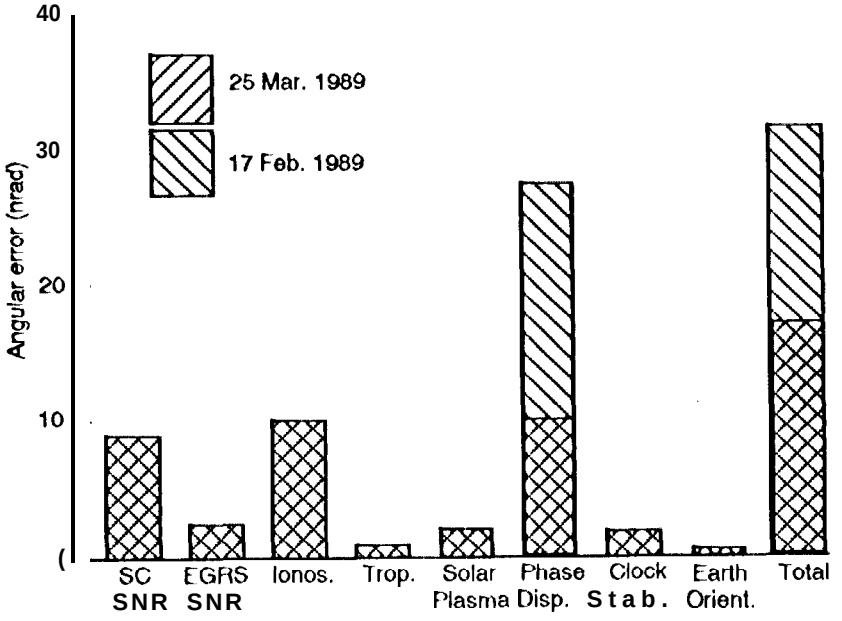

Figure 4. Major sources of error in the two ΔVLBI measurements of the Phobos 2 spacecraft.

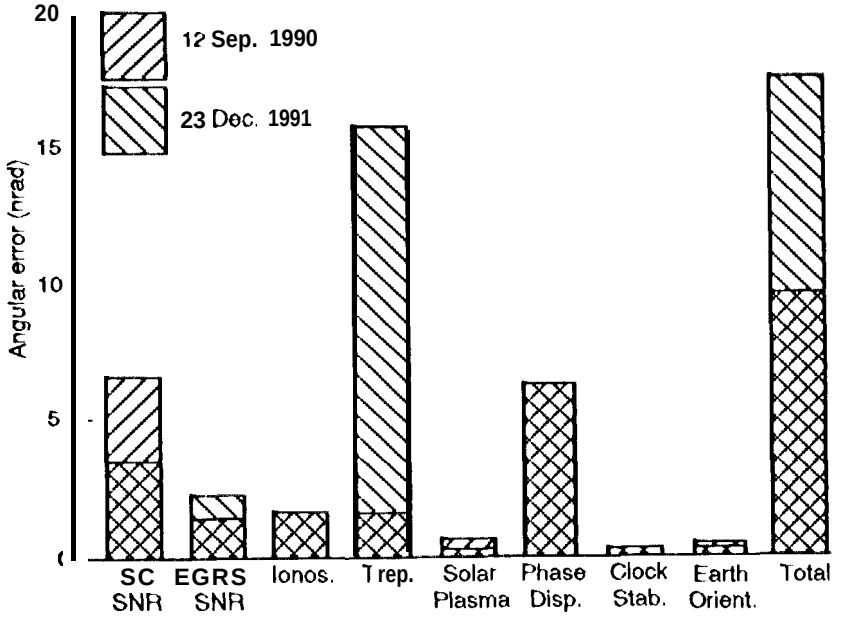

Figure 5. Major sources of error in 2 of the 4 ΔVLBI measurements of Magellan. Note the difference in the scale from Fig. 4.

System noise

The error from receiving system noise is primarily a function of the received signal strength for both the spacecraft and quasar signals, Estimates of this contribution are obtained during the post-processing phase of the analysis described earlier, In general the spacecraft signals for the Magel Ian observations are comparable to those observed for Phobos. The radio sources observed during the Phobos observations were, however, significantly weaker than the quasars observed during the Magellan observations. This resulted from attempts to reduce the ionosphere error in the Phobos observations by restricting the observed sources to those within a few degrees of the spacecraft, and these sources were often quite weak relative to the quasars used in the Magellan observations.

The AVI .BI observable is formed from the difference phase of the spacecraft and quasar signals. As described earlier, a correlation process extracts the phase from the recorded data at each antenna. In the case of the spacecraft signals, the correlat ion of the data recorded at each antenna is done independently using an accurate model of the spacecraft signal while the quasar correlation is done by a direct cross correlation of the sampled noise recorded at each antenna, In either case, the. uncerta inty in the phase of the correlated signal is given by:

$$\sigma_\phi = \frac{1}{SNR} \text{ (rad)} \tag{4}$$

where σ_ϕ is the. phase uncertainty and SNR is the correlation signal to noise ratio. The corresponding error in the AVI .BI delay is then given by

$$\sigma_\tau = \frac{2c\sigma_\phi}{W_{VLBI}} \text{ (cm)} \tag{5}$$

where W_{VLBI} is the spanned bandwidth of either the two spacecraft tones, or in the case of the quasar observation, the effective bandwidth of all channels. The factor of 2 in Eq. (3) accounts for the differencing between channels and stations that is done to compute the AVI .BI delay from the spacecraft and quasar delay observables.

Spacecraft SNR. It is the received phase of the spacecraft terms that is used to from the spacecraft dela y observable. Since the accuracy of the spacecraft delay observable depends on the spanned bandwidth of the spacecraft tones (Eq. (3)), as large a separation as possible is desired, However, because the power in the harmonics decreases with increasing separation from the carrier, the maximum spanned bandwidth is limited by the power in these harmonics. The signal to noise. ratio of the spacecraft tones is given by:

$$SNR = \sqrt{\frac{4P_r W_{ch} t_{obs}}{\pi k T_{sys}}} \tag{6}$$

where P_r is the received power, W_{ch} is the single channel bandwidth (1.8 MHz), t_{obs} is the length of the scan, and T_{sys} is the receiver system temperature., The received power is a function of the. distance between the spacecraft and Earth as given by

$$P_r = P_T g_T g_r \left(\frac{\lambda}{4\pi R}\right)^2$$

$$\text{“} \quad P_T g_r \left(\frac{r}{2R}\right)^2 (W) \tag{7}$$

where P_T is the transmitted power, g_T is the gain of the transmitting antenna, g, is the gain of the receiving antenna of cross sectional radius r, λ is the wavelength of the transmitted signal, and R is the distance from the antenna to the spacecraft, “l’he corresponding error in the difference delay (differenced between channels and stations) is

$$\sigma_\tau = \frac{c}{W_{VLBI}} \sqrt{\left(\frac{1}{2\pi SNR_2}\right)^2 + \left(\frac{1}{2\pi SNR_1}\right)^2} \tag{8}$$

where W_{VLBI} is the spanned bandwidth of the VI .BI tone.s, and the subscripts on the SNR terms refer to the two stations.

Quasar SNR. The signal to noise ratio of the correlated quasar signal for the VI.BI baseline is given by

$$SNR = 2.05 \times 10^{-4} D_1 D_2 s \sqrt{\frac{e_1 e_2 W_{ch} t_{obs}}{T_1 T_2}} \tag{9}$$

where D_1 and D_2 are the diameters of the two antennas, s is the source flux (Jansky), e_1 and e_2 are the efficiencies of the. two antennas, W_{ch} is the single channel bandwidth (2 MHz), t_{obs} is the. length of the scan, and T, and T_2 are the system temperatures of the two antennas. The factor of 2,05 x 10^{-4} is a collect ion of terms that accounts for the effects of two-level sampling, polarization, and includes the unit conversion factors. The signal to noise ratio for the delay formed by combining all of the single channels (i.e., the Bandwidth Synthesis Delay (BWS)) is them

$$\sigma_\tau = \frac{\sqrt{2}c}{2\pi W_{BWS} SNR_{ch}} \quad (cm) \tag{10}$$

where c is the speed of light, W_{BWS} is the effective spanned bandwidth, and SNR_{ch} is the single channel signal to noise ratio,

Ionosphere

As mentioned earlier, the ionosphere is a major source of error for the 1.-band Phobos 2 observations. The. effect of the ionosphere on radio frequency signals is to introduce an additional delay into the signal path from the spacecraft or quasar to the receiving antenna. This delay is a function of the frequency and the total integrated electron density along the ray path and is given by the relation[3]:

$$\tau_I = \frac{K? EC}{cf^2} \tag{11}$$

where τ_I is the additional delay due to the ionosphere in sec, TEC is the total integrated electron content (1 0^{16} electrons/m?), f is the frequency in Hertz, c is the speed of light, and κ is a constant equal to 40.3 in rnks units.

For the Phobos observations, estimates of the total electron content were available from Faraday rotation measurements at the DSN stations. These measurements provide estimates of the total electron content along a line of sight to a particular geosynchronous satellite, The total electron content along the Phobos or quasar line of sight is then determined from a spatial and temporal mode] for the ionosphere, It is uncertainty in this model which is the major source of error in the ionosphere delay calibrations.

The contribution of the ionosphere to the delay observable for the Magellan observations is much less than the Phobos observations, This is almost entirely due to the much higher frequency of the X-band Magellan observations which effectively reduces the ionospheric delay by over 90% relative to the I -band Phobos observations (Eq. 9), There are also improved ionospheric calibrations available for the Magellan observations that use signals broadcast by the constellation of Global Positioning System satellites to estimate the total electron content[4]. The wider coverage of the GPS satellites allows an improved estimate of the total electron content along the line of sight.

Solar plasma

The effect of the solar plasma on the passage of radio waves from the spacecraft to Earth is dependent on its location relative to the Sun. At Sun-Earth-probe (SEP) angles of less than 1 deg. it would be extremely difficult to track the phase of the spacecraft signals. At larger angles, the effect scales as the inverse sine of the SEP angle. atom-ding to the. relation[5]

$$\sigma_\tau = \frac{0.15\left(B/v_{sw}\right)^{.75}}{\nu^2\left[\sin\left(\theta_{sep}\right)\right]^{1.225}} \tag{12}$$

where B is the length of the projected baseline, v_{sw} is the velocity of the solar wind (400 km/sec), ν is the observing frequency and θ_{sep} is the Sun-Earth-probe angle.

Troposphere

Troposphere induced dcla y errors are composed of a static part due to both the wet and dry components of the troposphere and a fluctuating component attributed to the presence of water vapor. Calibration of the dry part of the static troposphere, obtained from surface meteorological measurements, is quite accurate, but there is likely to be a significant error due to the wet part of this component because of the inability of surface measurements to adequately estimate water vapor content at altitude. "l'his can be a serious error source for observations at low elevation angle and is given by

$$\sigma_\tau = \sigma_{zen}\left|\frac{1}{\sin\left(\theta_{sc}\right)} - \frac{1}{\sin\left(\theta_{sgra}\right)}\right| \tag{13}$$

where θ_{sc} is the elevation angle of the spacecraft observation and θ_{sgra} is the elevation angle of the quasar observation, and σ_{zen} is the residual error in the zenith static troposphere after cal i brat ion.

Treuhaft and Lanyi[6] have developed a model for the fluctuating component of the troposphere. Among the parameters of this model are the wind velocities at each observing site and the temporal separation of the scans, We have used this model to estimate the error induced by the fluctuating component of the troposphere, and find it to be a minor component of the total error budget.

Instrumental effects

Changes in the phase of the signals as they pass through the components of the receiving system before being digitized and recorded on tape introduce the most serious instrumental error in ΔVLBI observations. Although a large part of this error will difference between channels, stations and sources, even small errors in instrumental phase can result in a significant delay error given by

$$\sigma_\tau = \sqrt{2 \times 2 \times 2}\, c \frac{\sigma_\phi}{W_{VLBI}} \quad \text{(cm)} \tag{14}$$

where σ_ϕ is the residual phase dispersion error (after channel., station., and source differencing) in degrees, W_{VLBI} is the spanned bandwidth of the VLBI tones, and the 3 factors of the square root of 2 correspond to channel, station, and spacecraft-quasar delay differences. A further complica t ion arises from the fact that the spacecraft signal samples only a very narrow range of the phase response of each 2 MHz channel whereas the broadband noise signal of the quasar samples the entire bandpass of each channel. 'l'here is currently no system in place to provide phase calibration of narrow band signals such as those used for AV1 .BI measurements.

The other instrumental effect derives from the stability of the 1]-maser frequency standards at each site. The behavior of masers is well studied and a good model for the frequency stability is one of a "flicker" noise process, 'l'his results in an equivalent delay error given by

$$\sigma_\tau = \sqrt{2}\sigma_y\left(\tau = t_{sep}\right) \times t_{sep} \tag{1s}$$

where σ_y is derived from the Allen variance of the masers at each station and t_{sep} is the time interval between scans.

Earth orientation

Errors due to the uncertainty in the orientation of the AV1 .BI baseline in inertial space are caused by uncertainty in our knowledge of the Earth's rotation (UT1) and the two components of polar motion (Θ_x and Θ_y). There is also uncertainty in the *a priori* location of each tracking station. The errors in the baseline components due to these 3 sources arc given by[7]

$$\sigma^2_{B_X} = \left(\frac{B_Z}{r_p}\sigma_{\theta_X}\right)^2 + \left(\omega_e B_Y \sigma_{UT}\right)^2 + \sigma^2_X \tag{16}$$

$$\sigma_{B_Y}^2 = \left(\frac{B_Z}{r_p}\sigma_{\theta_Y}\right)^2 + \left(\omega_e B_X \sigma_{UT}\right)^2 + \sigma_Y^2 \tag{17}$$

$$\sigma_{B_Z}^2 = \left(\frac{B_X}{r_p}\sigma_{\theta_X}\right)^2 + \left(\frac{B_Z}{r_p}\sigma_{\theta_Y}\right)^2 + \sigma_Z^2 \tag{18}$$

where B_x, B_y, and B_z are the Cartesian baseline components, r_p is the Earth's polar radius, ω_e is the Earth's rotation rate, σ_{θ_x} and σ_{θ_y} are the uncertainties in the two components of polar motion, σ_{UT} is the uncertainty in Universal Time, and σ_X, σ_Y, and σ_Z are the *a priori* uncertainties in the baseline coordinates. The corresponding error in the. ΔVLBI delay is given by

$$\begin{aligned}\sigma_\tau = {} & \sigma_{B_X}\left|\sin\lambda_{sc}\cos\delta_{sc} - \sin\lambda_{egrs}\cos\delta_{egrs}\right| \\ & + \sigma_{B_Y}\left|\sin\lambda_{sc}\sin\delta_{sc} - \sin\lambda_{egrs}\sin\delta_{egrs}\right| \\ & + \sigma_{B_Z}\left|\sin\delta_{sc} - \sin\delta_{egrs}\right|\end{aligned} \tag{19}$$

where λ_{sc}, δ_{SC}, λ_{egrs}, and δ_{egrs} are the right ascension and declination of the spacecraft and the quasar respectively. Because of the availability of accurate measurements of polar motion, Earth rotation and station locations, this error source. is an insignificant portion of the ΔVLBI error budget.

RESULTS

A single. VLBI measurement of a planetary orbiter on a single baseline provides information on one component of the angular position of that spacecraft relative to a quasar. If the. spacecraft is a planetary orbiter and its position relative to the planet is known, then the position of the planet relative to the quasar can be estimated, What this information can reveal about the relationship between the planetary and radio reference frames depends upon how well the position of the planet is known in the reference frame of the planetary ephemerides. Table 2 lists the current uncertainties in the latitude. and longitude of the inner planets relative to Earth[8].

Table 2
RELATIVE ACCURACY OF PLANETARY POSITIONS

	Parameter uncertainty		
Planet	λ [a] *(1990), nrad*	ϕ,[b] *nrad*	*mean motion nrad/yr*[c]
Mercury	100	100	10
Venus	100	100	10
Mars	*5*	*2.5*	*0,5*

[a]Ecliptic longitude , [b]Ecliptic latitude,

Phobos

The. relative positions of Earth and Mars are well determined from ranging data to the Viking landers, which covered the period July, 1976 to November, 1982, From these data the ecliptic latitudes of Mars and Earth were determined to ~2 nrad and the relative ecliptic longitudes determined to ~5 nrad. The reference for ecliptic longitude is inferred from lunar laser ranging data, which is sensitive to the intersection of the Earth's equator and the ecliptic (the equinox). The ecliptic longitudes of Earth and Mars with respect to the. equinox of 1990 are known to ~5 nrad during the time of the Viking ranging data with a drift uncertainty of-15 nrad/decade.

The accuracy with which the relative positions of Earth and Mars arc known allows us to use the measured angular position of the Phobos spacecraft to estimate a meaningful value for the vector of rotations which describes the relation between the planetary and radio reference frames. Following *Finger and Folkner*,[9] the relation between the planetary and radio frame positions of a body is assumed to have the form

$$\vec{r}_R = \vec{r}_p - \vec{A} \times \vec{r}_p \qquad (20)$$

where $\mathbf{r_P}$ is the body's position in the planetary frame, $\mathbf{r_R}$ is the body's position in the radio frame, and **A is** a vector of three small rotation angles which describes the relationship between the two reference frames.

in order to accurately estimate all 3 components of the rotation vector A, a series of measurements distributed over a range of right ascension values is required. Because the Phobos 2 spacecraft was lost shortly after the second measurement in March 1989, only two components of the rotation vector can be estimated with useful precision. Figure 6 shows the definition of these two rotation angles. in this figure, the angles α and δ are approximately the right ascension and declination of Mars for the two measurements. Figure 7 shows estimates and uncertainties of these two angles based upon the Phobos 2 observations.

This result can be compared to an independent estimate of the frame tic rotation vector by *Finger and Folkner*.[9] Their work used a comparison of station locations determined from both VLBI and lunar laser ranging (LLR) data to estimate all three components of the frame tic rotation vector. Figure 7 shows both estimates of the two rotation angles along with their uncertainties.

Magellan

The position of Venus with respect to Earth is known to only ~25 nrad in ecliptic longitude and ~100 nrad in ecliptic latitude from planetary radar ranging data (which has an accuracy of ~50 m versus ~6 m for Viking ranging data). Because the.sc uncertainties are larger than our current knowledge the. rotation between the planetary and radio reference frames, the M agellan observations cannot be used to estimate. a useful value, for the. frame tic rotation. However, the 10-15 nrad precision of the Magellan ΔVLBI measurements can be used to greatly improve. our knowledge of the position of Venus in the radio reference frame and our knowledge of the angular position of Venus relative to earth, The results of these and any future. measurements will be provided to the ephemeris development group at the Jet Propulsion Laboratory for inclusion in the next version of the. planetary ephemeris.

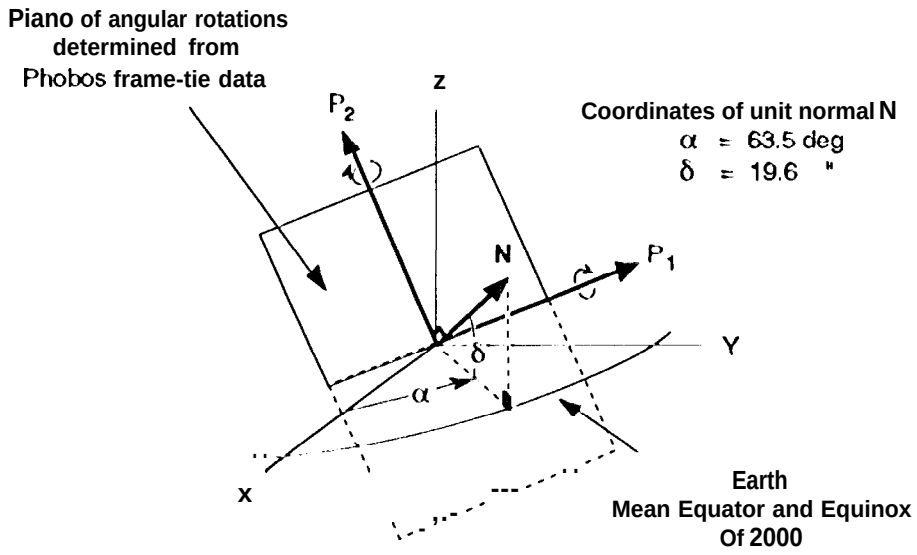

Figure 6. The definition of the frame tic rotation angles for the Phobos 2 observations.

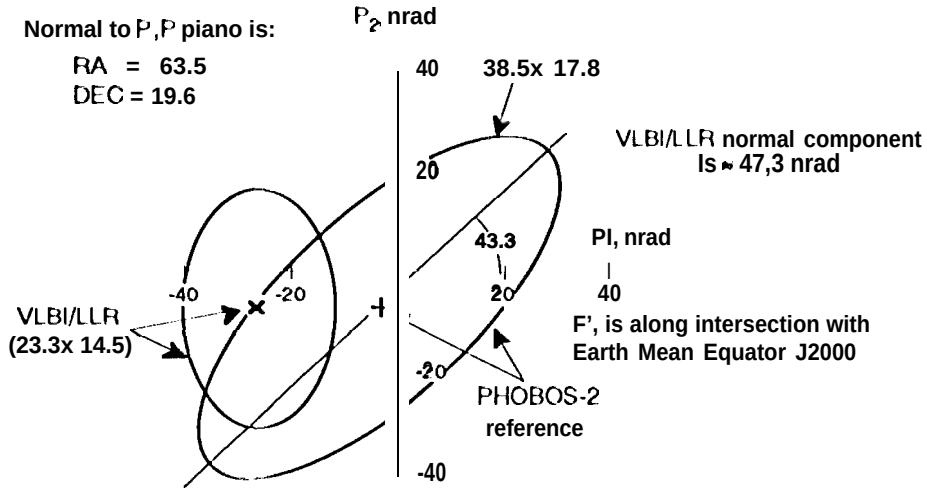

Figure 7. Comparison of estimates of the two rotation angles defined in Fig. 6 from the Phobos 2 observations and an independent determination by Finger and Folkner.

CONCLUSIONS

It is hoped that VI .BI observations of Magellan at Venus can continue. through the end of the mission (May 1993). Current problems with transmitters onboard the spacecraft, however, may curtail future observations. The next opportunity to make VI .BI measurements of a planetary orbiter will occur in late 1993 following the expected arrival of the Mars Observer spacecraft at Mars.

ACKNOWLEDGMENT

The research described in this paper was carried out by the Jet Propulsion laboratory, California Institute of '1'ethnology, under a contract with the National Aeronautic and Space Administration.

REFERENCES

1. O.J. Severs, "JPL 1990-3: A 5-nrad Extragalactic Source Catalog Based on Combined Radio 1 nterferometric Observations", *Telecommunications and Data Acquisition Progress Report 42-106,* Jet Propulsion Laboratory, Pasadena, California, 1991, pp. 364-383,

2. A. R. Thompson, J.W. Moran, and G.W. Swenson, Jr., "*Interferometry and Synthesis* in Radio *Astronomy*",John Wiley& Sons, 1986.

3. P.S. Callahan, "ionospheric Variations Affecting Altimeter Measurements: A Brief Synopsis", *Marine Geodesy,* Vol. 8, 1984, pp. 249-263,

4. G.E. Lanyi and T. Roth, 'A Comparison of Mapped and Measured Total Ionospheric Electron Content Using Global Positioning System and Beacon Satellite Observations", *Radio Science,* Vol. 23, No. 4, July-August 1988, pp. 438-492.

5. R.D. Kahn and J.S. Border, "Precise Interferometric Tracking of Spacecraft at Low Sun-Earth-Probe Angles", Paper AIAA-88-0572, Aerospace Sciences Meeting, Reno, NV, Jan 11-14, 1988.

6. R.N. Treuhaft and G.E. Lanyi, "The Effect of the Dynamic Wet Troposphere on Radio Interferometric Measurements", *Radio Science,* Vol. 22, 1987, pp. 251-275

7. J.G. Williams, ""Very Long Baseline Interferotmetry and Its Sensitivity to Geophysical and Astronomical Effects," *Space Program Summary 37-62, Vol. II,* Jet Propulsion Laboratory, Pasadena, California, March 1970, pp. 49-54.

8. E.M. Standish and J.G. Williams, "Dynamical Reference Frames in the Planetary and Earth-Moon Systems", *Inertial Coordinate Systems on the Sky,* Kluwer Academic Publishers, Dordrecht, 1990, pp. 173-181.

9. M.H. Finger and W.M. Folkner, "A Determination of the Radio-planetary Frame I-ie and the DSN Tracking Station Locations", *Proc. AIAA Astrodynamics Cent, 90-2905,* August 20-22, 1990.